MID-INFRARED (4.8 - 12.4 AND 20.0 μm) IMAGING OF THE GALACTIC CENTER: MODELING THE DUST EMISSION AND ENERGETICS OF THE CENTRAL PARSEC

DAN GEZARI, ELI DWEK AND FRANK VARROSI
NASA/Goddard Space Flight Center
Infrared Astrophysics Branch (Code 685)
Greenbelt, MD 20771

Abstract. We have modeled the mid-infrared emission from the Galactic Center using our array camera images at eight wavelengths. The results suggest that the high infrared luminosity of the region is provided by a cluster of luminous stars. There is no direct indication in the new model results of a very luminous object or "central engine" near Sgr A*.

1. Introduction

Two schools of thought have emerged which explain the high infrared luminosity and the apparent mass distribution in the Galactic Center. One contends that a recent episode of massive O star formation has occured (Rieke and Lebofsky 1982, Allen et al. 1990) which would account for the luminosity and ionizing radiation in the central few parsecs of the Galaxy. The other argues that the luminosity and central mass concentration are evidence for a "central engine" associated with Sgr A*, and that this object may be a massive black hole surrounded by an accretion disk (e.g. Lynden-Bell and Rees 1971, Rees 1982, Melia 1992).

The total infrared luminosity observed in the inner 2 parsecs of the Galactic Center is about 10^7 $L_\odot$ (Low et al. 1969, Becklin, Gatley and Werner 1982). There is evidence for the presence of a compact mass of $\approx 10^6$ $M_\odot$ within the central 0.1 pc (at or near Sgr A*) inferred from 12.8 μm Neon II emission line studies (Lacy et al. 1980) and 2.3 μm CO band observations (McGinn et al. 1989). These observations suggest that a very

L. Blitz and P. Teuben (eds.), Unsolved Problems of the Milky Way, 231–240.

energetic, compact object may exist at the nominal Galactic Center.

Several new results now make the idea of a single, exotic, luminous object at the Galactic Center seem somewhat less appealing. A cluster of luminous Helium I emission line stars has been detected in the central parsec (Krabbe et al. 1991, Krabbe 1993) which represent a significant source of luminosity for Sgr A West. These stars were found to be correlated with infrared brightness features and the details of the color temperature distribution (Gezari 1992). The modeling of the infrared emission presented here, using our new diffraction limited (1 arcsec resolution) array camera images at eight wavelengths between 4.8 and 20.0 μm, gives the distribution of dust temperature, emission opacity, line-of-sight extinction, and total infrared luminosity are computed over the central 15 arcsec field-of-view (1 parsec = 24 arcsec at 8.5 kpc), providing a basis for detailed analysis of the energetics and morphology of the central parsec of the Galaxy.

2. Instrumentation and Observations

The image data were obtained with the 58 x 62 pixel mid-infrared array camera developed at NASA/Goddard. The camera uses a gallium doped silicon (Si:Ga) direct readout (DRO) photoconductor detector array manufactured Hughes/Santa Barbara Research Center, with six fixed interference filters between 7.8 - 12.4 μm ($\Delta\lambda/\lambda = 0.1$). A complete description of the array camera system is presented by Gezari et al. (1992).

The structure of the core of Sgr A West at 12.4 μm is shown in Figure 1 and Color Plate 2, part of a large-scale 12.4 μm mosaic image of the Galactic Center was assembled from 50 individual array camera exposures. The images were made at the 3.0-meter NASA Infrared Telescope Facility (IRTF) at Mauna Kea, image quality was seeing-limited at typically 1.1 arcsec (FWHM) and pixel size was 0.26 arcsec. Point source positions can be measured to a relative astrometric accuracy of $\pm$ 0.1 arcsec. The mosaics are assembled using our MOSAIC image analysis software package (Varosi and Gezari 1993). An image set in eight colors between 4.8 and 20.0 μm (Figure 2) was obtained for the central 15 arcsec array field of view, each with typically 5 minutes of integration time. This data set provided low resolution spectra for each pixel position in the central $\approx$ 15 arcsec field of view, which were as input to the model.

3. Modeling the Infrared Emission

We have modeled the dust emission from the central parsec using the "stack" of eight 4.8 - 20.0 μm images, further constrained by 2.2 and 3.8 μm images by Herbst, Beckwith and Shure (1993). The spectrum for each 0.26 arcsec resolution element (pixel) within the field-of-view is obtained

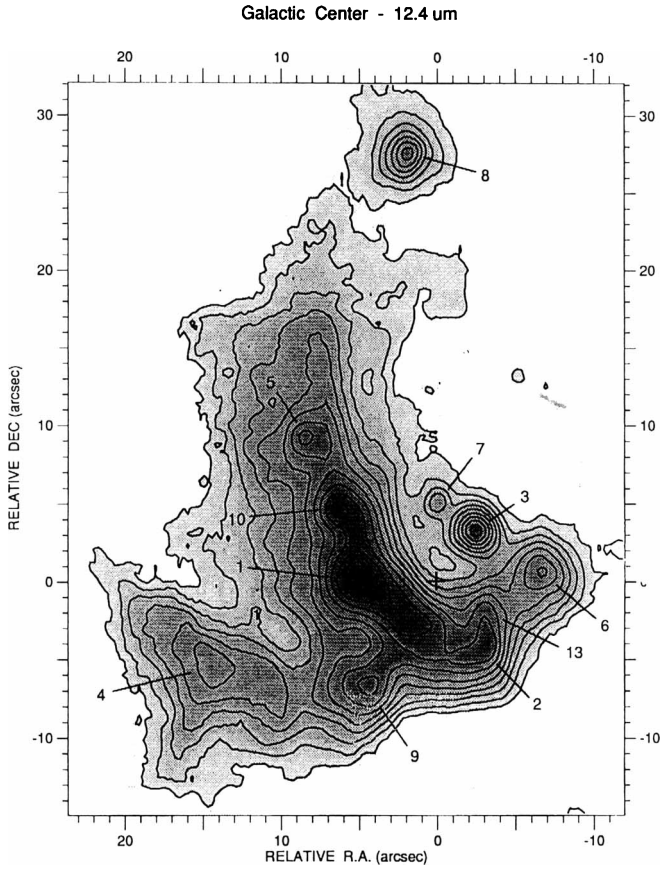

Figure 1. Contour map of the 12.4 μm continuum mosaic image of the Galactic Center Sgr A West complex obtained with our 58 x 62 Si:Ga array camera, developed at NASA/Goddard Space Flight Center (Gezari et al. 1992), at the 3-m NASA/IRTF Telescope at Mauna Kea. The mosaic was assembled from 50 overlapping 1 min integration frames (15 x 16 arcsec field of view, pixel size 0.26 arcsec), plotted with 30 contour intervals between the 3s noise level of 0.3 Jy/arcsec^2 and the peak brightness of 16 Jy/arcsec^2 at IRS 1. The prominent IRS sources are labled, and the cross shows the position of the non- thermal point source Sgr A* at the nominal Galactic Center. Deep integrations at 12.4 μm show no indication of infrared emission from Sgr A* (3s upper limit 0.1 Jy/arcsec^2 at 12.4 μm)

through the stack of aligned images. Because of limited spatial coverage at some wavelengths, the modeling calculations were restricted to an image overlap region common to all wavelengths of about 15 arcsec.

The spectrum of each pixel stack is modeled as arising from an isothermal source of mixed interstellar silicate and graphite dust, radiating at some temperature T. The emitted radiation is attenuated by an identical mixture of dust along the line of sight. Dust to gas mass ratios and dust

https://doi.org/10.1017/S0074180900229732 Published online by Cambridge University Press

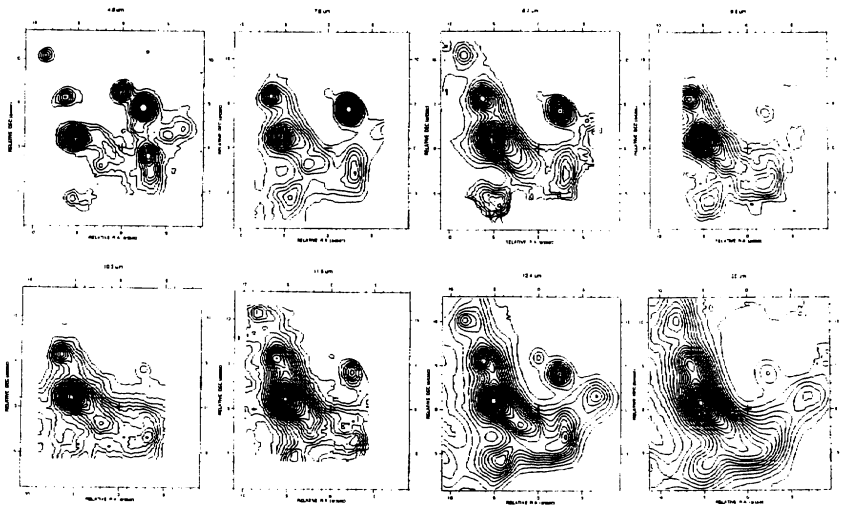

Figure 2. Galactic Center image set comprising the data "stack" used in the model, obtained with our 58 x 62 array camera. Top row: a) 4.8 μm. The ridge-like 4.8 μm emission just east of Sgr A* (cross) is the remnant of the IRS 16 cluster. b) 7.8 μm, c) 8.7 μm, and d) 9.8 μm array images. Local silicate extinction effects are dramatic at 9.8 μm; IRS 3 practically disappears in the image, where 95% of the 9.8 μm continuum flux is absorbed. The least silicate absorption is still very large, 80%, at IRS 1. Bottom row: e) 10.3 μm, f) 11.3 μm, g) 12.4 μm, and h) the 20.0 μm image, made with an Si:Sb array installed in the camera (Gezari et al. 1993).

optical constants were taken from Draine & Lee (1984). The observed infrared intensity I_ν from each source element (pixel) is then simply given by

$$I_\nu = (1 - e^{-\tau_S})B_\nu(T)e^{-\tau_{LOS}} \approx \tau_S B_\nu(T)e^{-\tau_{LOS}} (for \ \ \tau_S << 1)$$

where $\tau_S(\nu)$ is the source opacity of the emitting dust grains, $B_\nu(T)$ is the Planck function at the dust temperature T, and $\tau_{LOS}(\nu)$ is the line-of-sight (LOS) dust extinction opacity.

The model applies to the warm (T = 150 - 400 K) dust component in the galactic center region. Unfortunately, no high spatial resolution far-infrared photometry exists which could further constrain the fitting of model spectra longward of 20 μm. Despite this difficulty, model temperature resolution of 20K was achieved. We have not included 2.2 and 3.5 μm observations in our modeling, since strong sources in this wavelength range represent a different, much hotter dust component. The derived luminosity and dust mass results could be neglecting small contributions from cold (T $\approx$ 30 K) or hot (T > 400 K) dust not modeled. However, the color temperature

https://doi.org/10.1017/S0074180900229732 Published online by Cambridge University Press

calculated from the 2.2/4.8 μm flux ratio was considered when interpreting of the model results. More detailed description of the modeling effort will be presented by Gezari, Dwek, & Varosi (1994).

4. Results

The model results are presented in Figure 3(a-d). We find that IRS 1, 3, 5, 7, 10, 13, 21 and 29 all coincide with local peaks in the modeled dust temperature (Figure 3a) and are generally 100K warmer than the surrounding extended ridge material. IRS1 and IRS10 both have source temperatures T = 325K. IRS 13 is relatively warmer (T = 450K), as is IRS2 (T = 375K). The hottest sources are IRS 7 (T = 1300K), IRS3 (T = 600K), and the near infrared point source IRS29 (T = 600K) located 3 arcsec south of IRS3. The temperature peaks seem to be shifted slightly from the peaks of the IRS sources. It should be noted that positional shifts have been found (Gezari 1992) between the 12.4 μm IRS sources and the corresponding peaks in VLA 2-cm ionized gas maps, which could be interpreted as the influence of a central, luminous, ionizing source. These shifts are small, but real, well above the astrometric precision of the comparison.

The emitting dust (source) opacity distribution (Figure 3b) shows peaks which are anti-correlated with the 12.4 μm IRS sources. This contradicts the conclusion drawn by Gezari et al. (1985) that the observed infrared emission was due primarily to dust density structure. The present study resolves greater source detail, showing that the principal IRS sources are located between the opacity peaks, in regions of locally lower dust density. For the mixed silicate-graphite grain source case the peak 12.4 μm emission opacity in the region is $\tau_S \approx 0.3$, corresponding to a peak dust mass surface density of about 5×10^{-3} $M_\odot/arcsec^2$.

The opacity of extincting silicate-graphite dust along the line-of-sight is shown in Figure 3c. The extinction opacity distribution is rather smooth compared to the silicate feature strength image, with typical extinction opacity at 12.4 μm of about $\tau_{LOS} \approx 2$ across the extended ridge, peaking at $\tau_{LOS} = 2.5$ at IRS3. In the 9.8 μm silicate feature the extinction opacity is about $\tau_{LOS} \approx 4$ on the ridge, peaking at $\tau_{LOS} = 6$ at IRS3.

The model luminosity distribution result for the mixed silicate-graphite grain case (Figure 3d) shows peak values of 1×10^5 $L_\odot/arcsec^2$ at IRS1 and IRS3, and 5×10^4 $L_\odot/arcsec^2$ in typical regions of the extended ridge. The total luminosity integrated over the 15 arcsec (0.6 parsec) region modeled is about 5×10^6 $L_\odot$.

https://doi.org/10.1017/S0074180900229732 Published online by Cambridge University Press

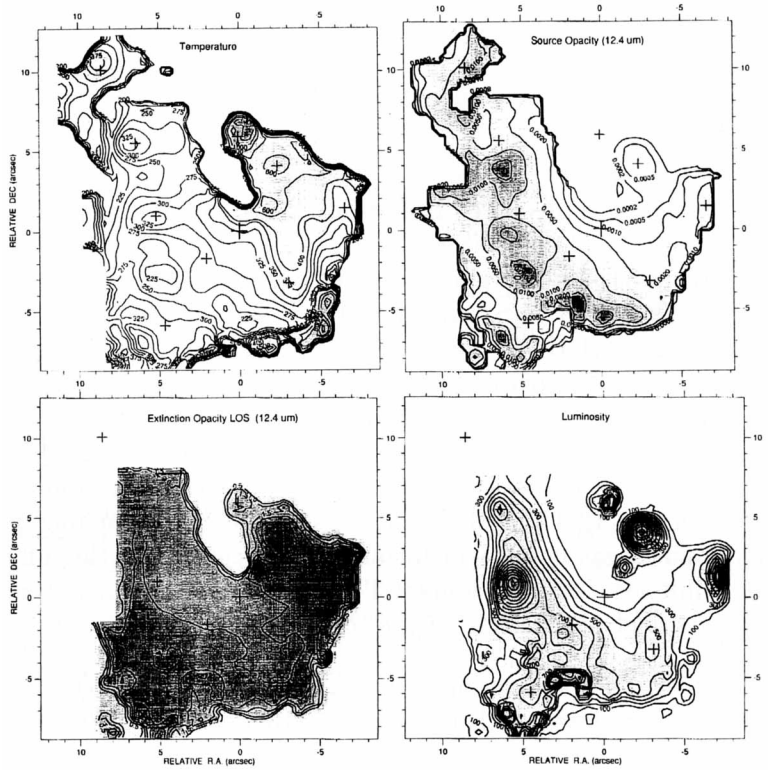

Figure 3. a) Dust temperature distribution modeled in the central 0.6 pc, calculated for mixed silicate-graphite grains. Darker colored regions are hotter. The positions of the IRS sources and Sgr A* are shown (crosses). Temperature enhancements are seen at the positions of the IRS sources, and correlations are seen at the positions of luminous Helium I line stars (see Figure 4). The model temperature is T = 325K at IRS1 and IRS10, and the hottest source is IRS7 where T = 1300K. b) Opacity of emitting dust grains showing anti-correlation with IRS source positions. Darker colored regions are more opaque, with peak opacity of $\tau_S \approx 0.3$ (or mass surface density 5×10^{-3} $M_\odot$/arcsec^2) close to IRS1, and minimum opacity level of $\tau_S \approx 0.02$. c) Extinction opacity of mixed silicate-graphite dust along the line-of-sight, with typical extinction opacity at 12.4 μm of about $\tau_{LOS} \approx 2$ across the extended ridge, peaking at $\tau_{LOS} = 2.5$ at IRS3. At 9.8 μm the extinction opacity is about $\tau_{LOS} \approx 4$ on the ridge, peaking at $\tau_{LOS} = 6$ at IRS3. d) Model luminosity distribution showing peak values of 1×10^5 $L_\odot$/arcsec^2 at IRS1 and IRS3, and 5×10^4 $L_\odot$/arcsec^2 in the extended ridge. The total luminosity integrated over the 15 arcsec (0.6 parsec) region modeled is about 5×10^6 $L_\odot$.

5. Discussion

The model results (temperature, opacity and luminosity distributions of the emitting dust) can be used in an attempt to discriminate between the "central engine" and "embedded stellar cluster" heating mechanisms. Since

https://doi.org/10.1017/S0074180900229732 Published online by Cambridge University Press

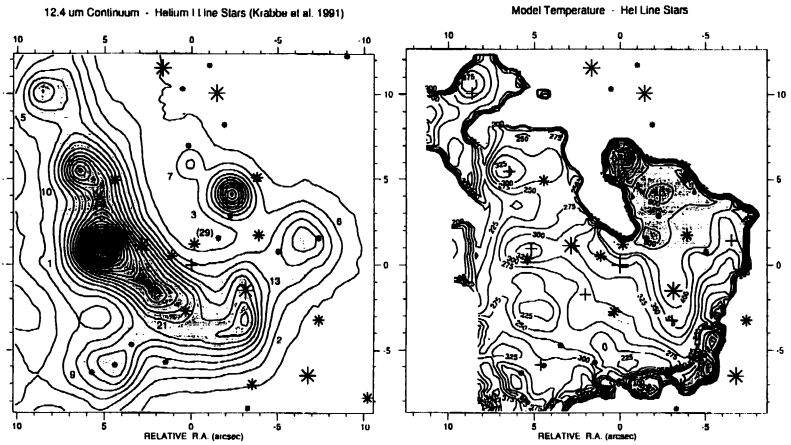

Figure 4. a) Positions of the more prominent Helium I emission line stars (asterisks, size proportional to brightness) in the central parsec found by Krabbe et al. (1991), shown with our 12.4 μm continuum brightness contours. These star data are new recent results provided by Krabbe (private communication). Positions are measured relative to Sgr A* (cross). b) Helium I star positions plotted on the modeled temperature distrubution of warm dust modeled in the Galactic Center. Darker regions are hotter. Note that the HeI stars are correlated with temperature enhancements, and occasionally with temperature minima in regions depleted of dust.

the source temperature distribution is determined by the density of the local ambient radiation field, a central luminosity source near Sgr A* should cause a large- scale temperature gradient radially across the extended infrared ridge, whereas embedded luminous stars should produce numerous local temperature "hot spots" throughout the ridge. The fact that the mid-infrared IRS sources all coincide with compact, symmetrical temperature peaks suggests that the IRS sources are heated by luminuos stars embedded at those positions, which is supported by the result that the dust density is lower near the IRS sources on the extended ridge (implying depletion of dust).

A detailed comparison between the positions of the HeI line stars imaged by Krabbe et al. (1991, 1993) and the mid-infrared model results shows that the HeI star positions are not well correlated with the compact 5 - 20 μm IRS source positions (see Figure 4a) or with the modeled source opacity and dust mass distributions (Figure 3b).

However, there is surprisingly good correlation between the HeI star positions and the modeled dust temperature features (Figure 4b). In almost every instance where the HeI stars lie in regions modeled, they are asso-

https://doi.org/10.1017/S0074180900229732 Published online by Cambridge University Press

ciated with local temperature enhancements or perturbations of the temperature contours. Considering the weakness of the correlation between the stars and dust density features, we conclude that the HeI stars are located between (rather than embedded within) the dense dust clouds in the Sgr A West complex. These stars would appear to heat the dust clouds externally, from dust-depleted regions between the IRS sources. But the HeI stars apparently are not embedded within the IRS sources themselves, which must contain other internal luminous objects.

The HeI stars are thought to be late-type blue supergiants stars (Najarro et al. 1993) with high mass-loss rates (10^{-5} to 10^{-4} $M_\odot$/yr) and high outflow velocities ($\approx$ 1000 km/s). These stars have predicted individual luminosities in the range $0.1 - 2 \times 10^6$ Lo resulting in a total luminosity of 1.2×10^7 $L_\odot$ for the entire $\approx$ 1 pc cluster (Krabbe et al. 1991). The new two-composition dust model fit indicates that the luminosity of all sources in the central 15 arcsec (0.6 pc) field-of-view modeled is 5×10^6 $L_\odot$, about half of the total infrared and far-infrared luminosity observed in the greater Sgr A West complex (central $\approx$ 2 parsecs). Thus radiation from the HeI emission line stars could account for the luminosity observed with the array camera from the central 15 arcsec field-of-view, and the total luminosity observed in the far infrared from the central few parsecs of the Galaxy.

We have seen that the compact IRS sources are warm spots in the dense Galactic Center dust complex. The temperature structure also suggests that the IRS sources contain embedded luminous stars which are not members of the HeI star cluster. The luminous HeI emission line stars must be co-located with the emitting dust in the Sgr A West infrared source complex, heating the dust clouds externally. However, there is little in the new model results to suggest the presence of a central luminosity source near Sgr A*. The weight of observational evidence thus seems to be falling on the side of luminous stars located in and among the dense dust clouds as the origin of the $\approx$ 10^7 $L_\odot$ luminosity. The present observational picture does not require that an exotic "central engine" be invoked to account for the high infrared luminosity of the Galactic Center.

Acknowledgements

This work was supported by NASA/OSS RTOPs 188-44-23-08 and 188-44-53-05.

References

Allen, D. A., Hyland, A. R., and Hillier, D. J. 1990, M. N. R. A. S., 244, 706.
Becklin, E. E., Gatley, I., and Werner, M. W. 1982, Ap. J., 258, 135.

Draine, B. T. and Lee, H. M. 1984, Ap. J., 285, 89.
Gezari, D. Y. 1992, in "The Center, Bulge and Disk of The Galaxy", ed. L. Blitz, Kleuwer Academic Publishers, Doecrecht, 23.
Gezari, D. Y., Dwek, E., and Varosi, F. 1994, (in preparation for Ap. J.).
Gezari, D. Y., W. Folz, L. Woods and Varosi, F. 1992, P. A. S. P., 104, 191.
Gezari, D. Y., Tresch-Fienberg, R., Fazio, G. G., Hoffmann, W. F., Gatley, I., Lamb, G., Shu, P., and McCreight, C. 1985, Ap. J., 299, 1007.
Gezari, Ozernoy, Varosi, McCreight, and Joyce 1993, "Nuclei of Normal Galaxies: Lessons Learned fronm the Galactic Center" ed. Genzel, R. and Harris, A., Kluwer Pub. Co. (Dordrecht), in press.
Herbst, R., Beckwith, S. V. W. and Shure, M. 1993, Ap. J. (Letters), 411, L21.
Krabbe, A., Genzel, R., Drapatz, S. and Rotaciuc, V. 1991, Ap. J. (Letters), 382, l19.
Krabbe, A. 1993 (private communication).
Lynden-Bell, D. and Rees, M. J. 1971, M. N. R. A. S., 152, 416.
McGinn, M. T., Becklin, E. E., Sellgren, K., and Hall, D. N. B. 1989, Ap. J., 338, 824.
Melia, F. 1992, Ap. J. (Letters), 387, L25.
Najarro, F., Hillier, D. J., Kudritzki, R. P., Krabbe, A., Genzel, R., Lutz, D., Drapatz, S., Geballe, T. R. 1993, Proc. "Nuclei of Normal Galaxies: Lessons Learned from the Galactic Center," ed. Genzel, R. and Harris, A., Kluwer Academic Pub. Co. (Dordrecht), in press.
Rees, M. J. 1982, "The Galactic Center", ed. G. Riegler and R. Blanford, American Institute of Physics, Conf. Series, 83, 166.
Rieke, G. H. and Lebofsky, M. J. 1982, "The Galactic Center", ed. G. Riegler and R. Blanford, American Institute of Physics, Conf. Series, 83, 194.
Varosi, F. and Gezari, D. Y. 1993, "Astronomical Data Analysis Software and Systems II", P. A. S. P. Conf. Series, 52, 393.

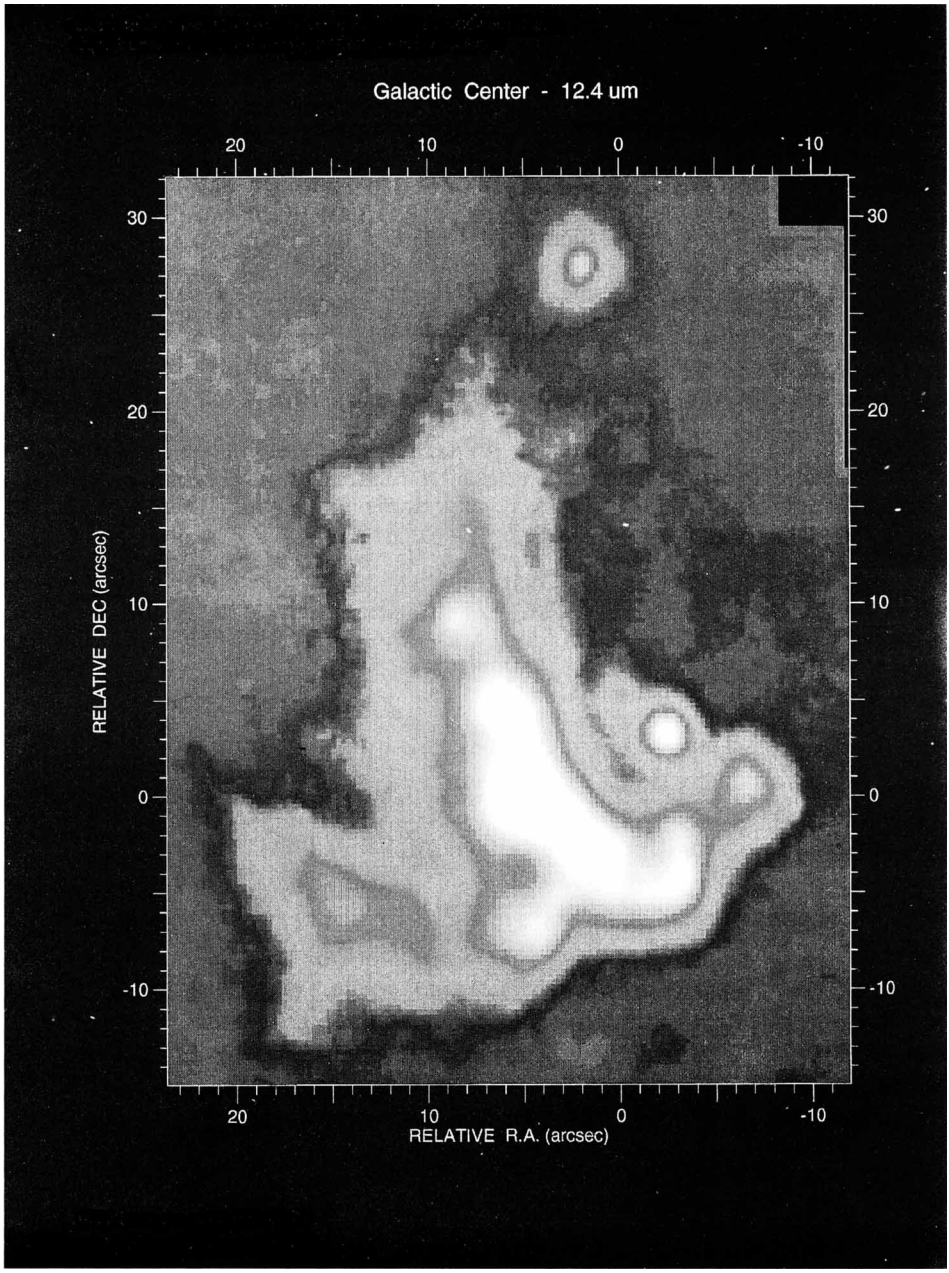

Figure 2. 12.4 μm continuum mosaic of the central 2 pc of the Galactic Center Sgr A West complex obtained with the 58 x 62 array camera (Gezari et al. 1992) at the 3-m NASA/IRTF Telescope at Mauna Kea. The intensity display is logarithmic to show details in regions of extended faint emission. The mosaic was assembled from 50 overlapping 1 min integration frames (15 x 16 arcsec field of view, pixel size 0.26 arcsec) which were aligned, matched and coadded to make up the final mosaic. Positions are measured relative to Sgr A*. The strongest infrared emission is very similar to the ionized gas distribution observed in 2-cm and 6-cm VLA maps of the region.

(For colour plate of figure see page xix)

https://doi.org/10.1017/S0074180900229732 Published online by Cambridge University Press